ISSN 1027-4510, *Journal of Surface Investigation: X-ray, Synchrotron and Neutron Techniques, 2024, Vol. 18, No. 5, pp. 1072–1077. © Pleiades Publishing, Ltd., 2024.*

Synthesis of Hydride Phases Based on TiZrNbMoTa High-Entropy Alloy

S. A. Lushnikov[a], * and T. V. Filippova[a]
[a] *Moscow State University, Moscow, 119991 Russia*
**e-mail: lushnikov@hydride.chem.msu.ru*

Received January 28, 2024; revised February 22, 2024; accepted February 22, 2024

Abstract—A high-entropy TiZrNbMoTa alloy with a body-centered cubic lattice has been synthesized. The interaction of the alloy with hydrogen is accompanied by the formation of samples containing hydride phases with tetragonal and cubic lattices. Hydrogen desorption from the hydride at a high temperature leads to the formation of a fine metal powder of the original alloy with the cubic lattice. Samples of the alloy and hydride phases are analyzed by X-ray diffraction and electron microscopy.

Keywords: high-entropy alloys, hydride phases, X-ray diffraction

DOI: 10.1134/S102745102470085X

INTRODUCTION

Currently, a group of high-entropy alloys is the object of active research because they have valuable properties that are in demand for practical use [1–14]. For example, it can be noted that high-entropy alloys are characterized by high heat resistance, wear resistance, and corrosion resistance. Alloys with niobium are biologically compatible with the human body and are potential materials for implants [13]. No less interesting is the study of the interaction of high-entropy alloys with hydrogen and the synthesis of hydride phases based on them [15–18]. After hydrogen desorption from hydride phases at elevated temperatures, as a rule, fine metal powders of the original alloys are formed. This material significantly expands the range of practical applications of high-entropy alloys, since it allows coating various products with a thin layer of the alloy in powder form. The structure of high-entropy alloys is a crystal lattice, in the nodes of which various metal atoms are statistically distributed in an equiatomic ratio. The most typical representatives of high-entropy alloys are alloys with a body-centered cubic (bcc) lattice containing atoms of titanium, zirconium, molybdenum, and niobium. No less important are iron-based alloys containing nickel, chromium, manganese, and vanadium, which have high resistance to mechanical wear and corrosion. In this work, we studied hydride phases based on the high-entropy TiZrNbMoTa alloy with the bcc lattice and samples of the alloy after hydrogen desorption. This alloy is close in composition to prototypes of biocompatible alloys, and obtaining it in the form of a fine powder significantly expands the scope of practical application and reduces the cost of products.

EXPERIMENTAL

A sample of the high-entropy alloy TiZrNbMoTa was prepared from high-purity metals by melting in an electric arc furnace in an argon atmosphere. The synthesis of hydride phases was carried out in a Sieverts-type installation with a hydrogen pressure range of up to 10 MPa. The amount of hydrogen in the formed hydrides was calculated using the volumetric method using the van der Waals equation for real gases. Samples of alloys and hydride phases were studied by X-ray phase analysis (XPA) on a Rigaku M2500 diffractometer with a copper anode. The chemical composition of the sample was monitored using a Tescan VEGA3 LMU scanning electron microscope. The phase composition of the samples was refined by the Rietveld method.

RESULTS AND DISCUSSION

According to the X-ray diffraction data, a sample of the TiZrNbMoTa alloy is single-phase with the bcc lattice, space group (sp. gr.) $Im\bar{3}m$ (No. 229) (Fig. 1, Table 1). The results of electron microscopy confirmed that the chemical composition of the sample corresponds to the formula TiZrNbMoTa. The interaction of hydrogen with the TiZrNbMoTa alloy at a pressure of 20 bar and room temperature leads to the formation of a hydride phase. At the end of the synthesis, the autoclave with the sample was cooled to the temperature of liquid nitrogen and again heated to room temperature. The sample of the hydride phase obtained in this way contained an amount of hydrogen corresponding to 0.9 hydrogen atoms per metal atom of the crystal lattice. X-ray diffraction analysis of the

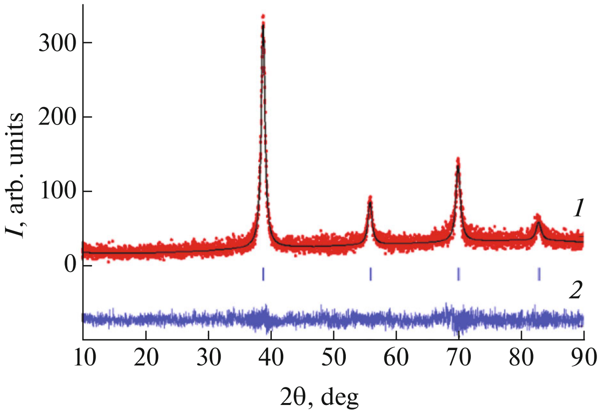

Fig. 1. X-ray diffraction pattern of TiZrNbMoTa processed by the Rietveld method: experimental (dots) and calculated profiles (solid line) (*1*) and the difference between them (*2*). The dashes correspond to Bragg positions.

synthesized hydride sample showed (Fig. 2, Table 1) that it consists of two phases—with a tetragonal lattice (70%) and a weakly expanded bcc lattice (30%). A phase with the tetragonal lattice is formed during the hydride formation reaction; the cubic lattice of the original alloy (sp. gr. $Im\bar{3}m$) transforms into the tetragonal one (sp. gr. $I4/mmm$ (no. 139)) (Fig. 3). A similar transformation of the cubic lattice into the tetragonal one during hydride formation was also discovered in the case of the high-entropy TiVZrNbHf alloy [15]. The resulting hydride phase absorbed approximately the same amount of hydrogen (less than 1.0 hydrogen atom per lattice metal atom), as well as the TiZrNbMoTa-based hydride synthesized in this work. Additionally, the authors of [15] found that with a further increase in hydrogen concentration, a new transformation of the crystal lattice from the tetragonal to face-centered cubic (fcc) is observed. This transition occurs when the amount of hydrogen in the hydride phase reaches close to 2.0 hydrogen atoms per lattice metal atom. In the sample under study, the second hydride phase with a cubic expanded lattice is a solid solution of hydrogen in the original alloy. The crystal lattice of the cubic phase is slightly expanded, and the relative increase in volume $\Delta V/V$ amounted to about 4.0% (Table 1). The weak lattice expansion allows us to conclude that the amount of hydrogen in the cubic phase is insignificant. Resynthesis of a hydride based on the high-entropy TiZrNbMoTa alloy at elevated hydrogen pressure (40 bar) and room temperature also leads to the formation of a hydride containing a phase with tetragonal and expanded cubic lattices. The amount of hydride phase in the sample became less (about 40%) than that in the case of a similar hydride after cooling to a low temperature. The newly formed hydride phase contains approximately the same amount of hydrogen corresponding to 0.9 hydrogen atom per lattice metal atom. Thus, the hydride formation reaction in the case under consideration leads to the formation of samples containing two phases.

This behavior may be caused by the structural features of the bcc crystal lattice, in the interstices of which hydrogen atoms are introduced. Study of the structure of d-metal hydrides with the bcc lattice using neutron diffraction [19] made it possible to establish that hydrogen atoms can fill interstices of two types—tetrahedral and octahedral. The complete occupation of interstitial sites of any type in the lattice is prevented by long-range interaction between hydrogen atoms, the so-called interstitial blocking effect. This effect manifests itself in the fact that in the crystal lattice the interstices closest to the occupied hydrogen atom remain vacant. It was experimentally established that the blocking effect is most pronounced at a distance of about 2.1 Å and decreases as this distance increases. Therefore, it can be assumed that a distance of 2.1 Å is the minimum between hydrogen atoms in the metal sublattice of the hydride and does not depend on the type of metal atoms. In addition, [9], the authors of [9] came to the conclusion that one of the factors determining the tetrahedral or octahedral coordination of hydrogen atoms in d-metal hydrides is a geometric criterion, such as the radius of the metal atoms of the lat-

Table 1. Lattice parameters of alloy samples, hydride phase, and samples after hydrogen desorption

Samples	Lattice parameters				Synthesis conditions: p, T, amount of hydrogen
	a, nm	s, nm	V, 10^{-3} nm^3	$\Delta V/V$, %	
TiVZrNbHf alloy [8]	0.3659(3)	–	48.9	–	Melting
TiZrNbMoTa alloy	0.3343(3)	–	37.4	–	Melting
TiZrNbMoTa hydride phase	0.3388(2)	–	38.9	4.0	20 bar, 295 K, 0.9 hydrogen atoms per metal atom
	0.3197(2)	0.4568(3)	46.7	24.9	
TiZrHfMoTa powder	0.3397(3)	–	39.2	4.8	Desorption at 673 K
TiZrHfMoTa powder	0.3369(3)	–	38.2	2.1	Desorption at 773 K
TiZrHfMoTa powder	0.3354(3)	–	37.7	0.8	Desorption at 973 K

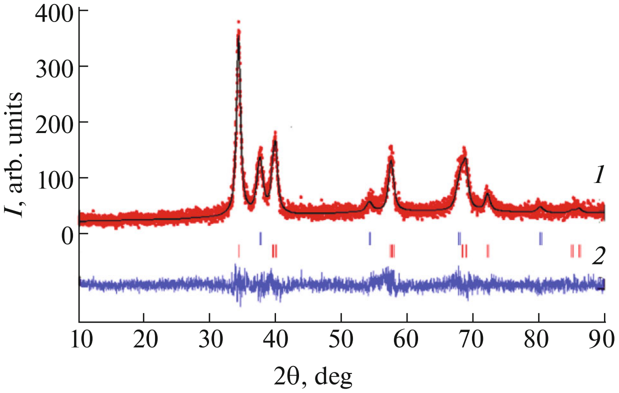

Fig. 2. X-ray diffraction pattern of the TiZrNbMoTa-based hydride phase with an amount of hydrogen of 0.9 atoms per lattice metal atom processed by the Rietveld method: experimental (dots) and calculated profiles (solid line) (*1*) and the difference between them (*2*). The dashes correspond to Bragg positions: the top row is the hydride phase with the cubic lattice, and the bottom row is with the tetragonal lattice.

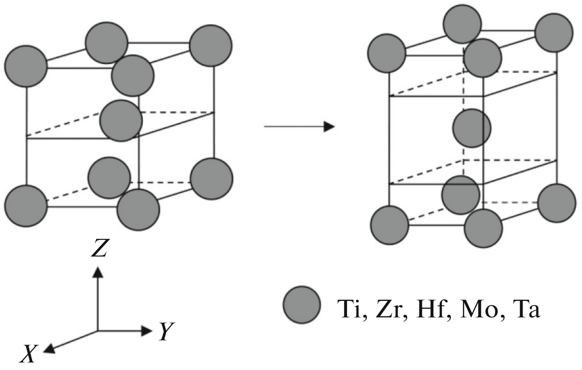

Fig. 3. Transformation of the crystal lattice of the TiZrNbMoTa alloy from bcc (left) to tetragonal (right) during hydride formation.

tice or its period. In lattices with large radii of metal atoms, such as titanium, zirconium, and hafnium, hydrogen prefers to fill tetrahedral interstices. In metal lattices of chromium, nickel, and iron with a small atomic radius, the coordination of hydrogen is octahedral. The peculiarity of the lattice of vanadium atoms is that it allows simultaneous filling of interstices of both types. High-entropy alloys with the bcc lattice are also attractive because in them, along with tetrahedral interstices, hydrogen can simultaneously fill octahedral ones. First of all, this is possible in lattices with metal atoms of a sufficiently large radius and, accordingly, with an increased period, such as, for example, scandium, titanium, and hafnium. In this case, increased interatomic distances in the lattice make it possible to avoid the blocking effect.

Along with the geometric parameters of the lattice, it is also necessary to take into account that the volume that a hydrogen atom contributes to the lattice may be different. This means that the hydride formation reaction leads to the appearance of various volumetric lattice effects. As was established in [20, 21], such effects are determined primarily by the type of metal atoms in the crystal lattice. The authors of [20] discovered that the volumetric expansion of the crystal lattice during the formation of *d*-metal hydrides can be very large, as, for example, in the case of the atoms of niobium, tantalum, and nickel. On the contrary, for titanium, hafnium, and manganese atoms the lattice expansion is much smaller, and this trend in both cases is observed at similar hydrogen concentrations in the hydride. As was shown in this work, this behavior is caused by the fact that the volume contributed by the hydrogen atom to the lattice consists of geometric and additional volumes. The geometric volume is determined by the radius of a free hydrogen atom (close to 0.055–0.057 nm) and corresponds to 2.7×10^{-3} nm^3. The additional volume significantly depends on the interaction of the electron density of the hydrogen atom in interstices with electrons of the *d*-band of metal atoms surrounding these interstices. Since, when occupying an interstitial site in the lattice, a hydrogen atom partially donates its electron to *d*-band of metal atoms, its radius (0.055–0.057 nm) decreases. Therefore, additional volume always reduces a value of 2.7×10^{-3} nm^3 of the geometric volume; this reduction can reach up to 30% and depends on the electronic characteristics of the metal atoms of the lattice. The interaction of hydrogen and lattice metal atoms is determined by the density of spin states of the *d*-band of metal atoms on the Fermi surface [20], which varies unevenly over the period of the periodic table. If *d*-sublevel is filled with unpaired electrons and the density of spin states is low (typical for metals of groups IV, VII), then the additional volume is large and the volumetric expansion of the lattice decreases due to a decrease in the geometric volume. This occurs because the hydrogen atom has transferred a significant portion of its electron density to the *d*-band of metal atoms, and its radius decreased. At high densities of spin states (metals of groups V, VIII), when *d*-sublevel is almost completely populated by paired electrons; the hydrogen atom can practically no longer donate its electron density there. The additional volume decreases sharply, the geometric volume increases, approaching a maximum value of 2.7×10^{-3} nm^3, and the hydride lattice expands as much as possible. Thus, to reduce the blocking effect, it is necessary to take into account not only the radius of the metal atoms that make up the components of the alloy but also the type of these atoms, which can cause different volumetric effects in the crystal lattice of the hydride phases.

As was mentioned in [15], in the case of the formation of hydride phases based on an alloy with the bcc lattice TiVZrNbHf (a = 0.3659 nm) the lattice type

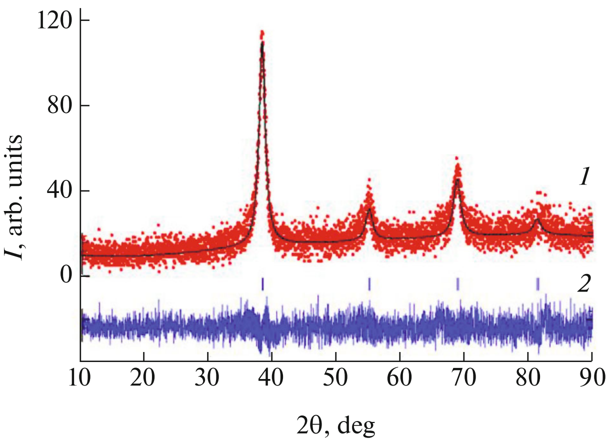

Fig. 4. X-ray diffraction pattern of the TiZrNbMoTa-based hydride phase after hydrogen desorption at a temperature of 673 K processed by the Rietveld method: experimental (dots) and calculated profiles (solid line) (*1*), and the difference between them (*2*). The dashes correspond to Bragg positions.

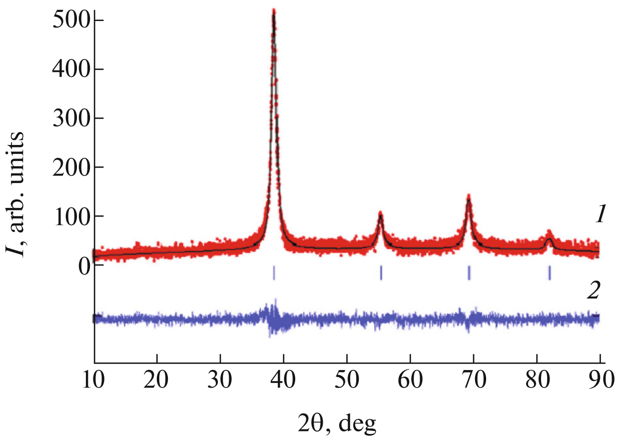

Fig. 5. X-ray diffraction pattern of the TiZrNbMoTa-based hydride phase after hydrogen desorption at a temperature of 773 K processed by the Rietveld method: experimental (dots) and calculated profiles (top line) (*1*) and the difference between them (*2*). The dashes correspond to Bragg positions.

changes from bcc to tetragonal and fcc. A similar transformation is observed for hydride phases of *d*-metals whose saturated hydrides have the fcc lattice. In the case of a crystal lattice with a short period, the filling of interstices in the lattice with hydrogen is significantly influenced by the blocking effect. Therefore, the lattice transformation from bcc to fcc can be inhibited, and even the decomposition of the hydride sample into two phases is possible [19]. This process is apparently observed with the hydride phase based on the TiZrNbMoTa alloy and the lattice parameter a = 0.3343 nm less than that of the TiVZrNbHf alloy (a = 0.3659 nm). In this case, the phase transition from the bcc lattice was not complete and hydride formation was completed with the formation of a two-phase sample with a tetragonal and expanded bcc lattice. To reduce the blocking effect, it is necessary to try to select alloy components from metals with a large atomic radius. This will increase the distance between voids of both tetrahedral and octahedral types. To achieve this goal, in the TiZrNbMoTa alloy, molybdenum, which has the smallest atomic radius of all alloy components, can be replaced by other metals, such as hafnium, scandium, or tungsten. A comparison of the type of metal atoms in the TiZrNbMoTa and TiVZrNbHf alloys [15] showed that in both cases the volumetric effects of hydride formation are approximately the same. This follows from a comparison of vanadium and tantalum atoms and a pair of hafnium and molybdenum atoms, for which such effects are close [20]. Thus, the determining factor when choosing alloy components, which reduces the blocking effect during hydride formation, is the choice of metals with a large atomic radius, which increase the lattice parameter. It can also be noted that the fcc lattice parameter of the hydride phase is increased compared to the bcc lattice parameter of the original alloy. This lattice change can also help overcome the interstitial blocking effect and fill both types of voids in the metal hydride matrix. To confirm these assumptions, it is necessary to conduct a neutron diffraction study of hydride phases. This will make it possible to experimentally determine the types and occupancy of positions in the metal matrix of the hydride phase.

The obtained samples of hydride phases based on the TiZrNbMoTa alloy studied in this work are fine metal powders containing hydrogen. To remove hydrogen, the hydride sample was desorbed at high temperature in vacuum for 1 h, taking into account that too high a temperature can lead to the disproportionation reaction and decomposition of the metal hydride matrix into individual components. The first sample of hydride powder was desorbed at a temperature of 673 K. XPA data showed that the sample after desorption has a weakly expanded bcc-type lattice, the same as that of the original alloy with a relative increase in volume $\Delta V/V$ amounting to 4.8% (Table 1). In the diffraction pattern of the sample (Fig. 4), one can note an increased background and low intensity and broadening of the peaks, which indicates poor crystallinity of the powder. The presence of weak lattice expansion and low crystallinity confirm that at this temperature desorption was not complete and a small amount of hydrogen remained in the sample. The next hydride sample was desorbed at a higher temperature of 773 K. In the diffraction pattern of the sample after hydrogen desorption, one can notice a significant improvement in the crystallinity of the

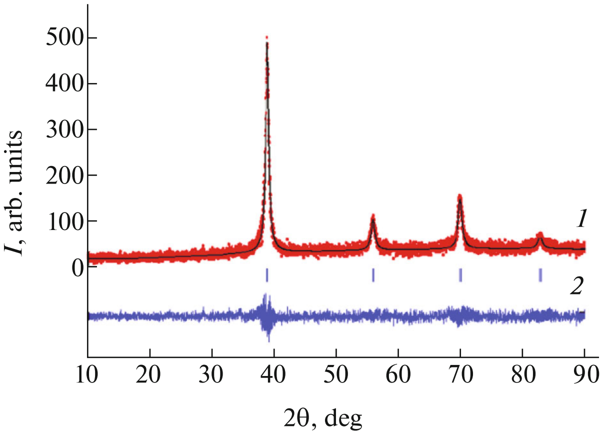

Fig. 6. X-ray diffraction pattern of the TiZrNbMoTa-based hydride phase after hydrogen desorption at a temperature of 973 K processed by the Rietveld method. The experimental (dots) and calculated profiles (solid line) (*1*), and the difference between them (*2*). The dashes correspond to Bragg positions.

powder—narrow peaks with high intensity and low background appeared (Fig. 5). Increase in relative lattice volume $\Delta V/V$ is insignificant and amounts to 2.1%. Another sample of the hydride phase powder was desorbed at a temperature of 973 K. In the diffraction pattern of this sample, only a slight improvement in the crystallinity of the powder can be seen (Fig. 6). Increase in relative lattice volume $\Delta V/V$ is barely noticeable and amounts to 0.8%. This indicates that there is virtually no hydrogen left in the sample. Thus, the desorption of hydrogen from samples of the hydride phase based on the TiZrNbMoTa alloy at elevated temperatures leads to the formation of fine metal powder of the original alloy with traces of hydrogen.

CONCLUSIONS

The hydride phase has been synthesized based on the high-entropy alloy with the bcc lattice TiZrNbMoTa with an amount of hydrogen close to 0.9 hydrogen atom per lattice metal atom. It was found that after the hydride formation reaction the resulting samples contain two hydride phases with tetragonal and expanded bcc lattices. The two-phase samples apparently formed since hydrogen atoms, due to the blocking effect, filled only part of the interstices in the lattice. Moderate temperatures of hydrogen desorption from the synthesized hydride phases make it possible to obtain finely dispersed metal powder of the initial high-entropy alloy TiZrNbMoTa. Its crystallinity depends on the temperature at which hydrogen desorption is carried out.

FUNDING

The work was carried out within scientific program of the National Center for Physics and Mathematics (direction no. 8 “Physics of hydrogen isotopes”, 2023—2025).

CONFLICT OF INTEREST

The authors of this work declare that they have no conflicts of interest.

REFERENCES

1. D. B. Miracle and O. N. Senkov, Acta Mater. **122**, 448 (2017). https://doi.org/10.1016/j.actamat.2016.08.081
2. Z. Q. Xu, Z. L. Ma, M. Wang, Y. W. Chen, and Y. D. Tan, Mater. Sci. Eng. A **755** (7) 925 (2019). https://doi.org/10.1126/science.abe5323
3. S. Son, D. Lee, H. Kwon, J. Moon, K. B. Park, A. Kim, J. Choi, J.-H. Jeong, S. Cho, and H. S. Kim, J. Alloys Compd. **935**, 168089 (2023). https://doi.org/10.1016/j.jallcom.2022.168089
4. K. Yao, Y. Zhang, L. Liu, X. Zhang, K. Duan, B. Liu, J. Qi, Z. Zhao, and F. Wu, J. Alloys Compd. **947**, 169616 (2023). https://doi.org/10.1016/j.jallcom.2022.168089
5. X. Yan and Y. Zhang, Scr. Mater. **178**, 329 (2020). https://doi.org/10.1016/j.scriptamat.2019.11.059
6. H. Shen, J. Zhang, J. Hu, J. Zhang, Y. Mao, H. Xiao, X. Zhou, and X. Zu, Nanomaterials **9**, 248 (2019). https://doi.org/10.3390/nano90202482
7. V. F. Gorban, N. A. Krapivka, S. A. Firstova, and D. V. Kurilenkoa, Phys. Met. Metallogr. **119** (5), 477 (2018). https://doi.org/10.1134/S0031918X18050046
8. X. H. Yan, J. S. Li, W. R. Zhang, and Y. Zhang, Mater. Chem. Phys. **210**, 12 (2018). https://doi.org/10.1016/j.matchemphys.2017.07.078
9. A. A. Rempel and B. R. Gel’chinskii, Izv. Ferrous Metall. **63** (3–4), 248 (2020). https://doi.org/10.17073/0368-0797-2020-3-4-248-253
10. I. Kunce, M. Polanski, and J. Bystrzycki, Int. J. Hydrogen Energy **38** (27), 12180 (2013). https://doi.org/10.1016/j.ijhydene.2013.05.071
11. W. Kucza, J. Alloys Compd. **894**, 162443 (2022). https://doi.org/10.1016/j.jallcom.2021.162443
12. Y. Zhang, Y. J. Zhou, J. P. Lin, G. L. Chen, and P. K. Liaw, Adv. Eng. Mater. **10**, 534 (2008). https://doi.org/10.1002/adem.200700240
13. L. C. Zhang and L. Yu. Chen, Adv. Eng. Mater **21**, 1801215 (2019). https://doi.org/10.1002/adem.201801215
14. F. Pineda, C. Martinez, P. Martin, and C. Aguilar, Rev. Adv. Mater. Sci. **62**, 1 (2023). https://doi.org/10.1515/rams-2023-0150
15. C. Zlotea, M. A. Sow, G. Ek, J. P. Couzinie, L. Perriere, I. Guillot, J. Bourgon, K. T. Moller, T. R. Jensen,

and E. Akiba, J. Alloys. Compd. **775**, 667 (2019). https://doi.org/10.1016/j.jallcom.2018.10.108

16. H. Luo, Z. Li, and D. Raabe, Sci. Rep. **29** (7 (1)), 9892 (2017). https://doi.org/10.1038/s41598-017-10774-4
17. M. M. Nygårda, W. A. Sławinski, G. Ekc, M. H. Sørbya, M. Sahlbergc, D. A. Keend, and B. C. Hauback, Acta Materialia **199**, 540 (2020). https://doi.org/10.1016/j.actamat.2020.08.045
18. C. Zlotea, M. A. Sow, G. Ek, J.-P. Couzinié, et al., J. Alloys Compd. **775**, 667 (2019). https://doi.org/10.1016/j.jallcom.2018.10.108
19. V. A. Somenkov, Ber. Bunsen-Ges. Phys. Chem. **76**, 733 (1972). https://doi.org/10.1002/CHIN.197247005
20. V. A. Somenkov and S. Sh. Shil'shtein, Fiz. Met. Metalloved. **65** (1), 132 (1988).
21. V. A. Somenkov and S. Sh. Shil'shtein, Fiz. Met. Metalloved. **86** (3), 114 (1998).